Molecular Crystals and Liquid Crystals
Publication details, including instructions for authors and subscription information:
http://www.tandfonline.com/loi/gmcl16

Superconducting Lenses for Steric Structure Determination of Organic Material in the Electron Microscope

Erwin Knapek [a], Guy Lefranc [a], Wolfgang v. Gentzkow [a], Isolde Dietrich [a] & Helmut Formanek [b]
[a] Zentrale Forschung und Entwicklung, Siemens AG, D-8000 München, Postfach, 830 952
[b] Botanisches Institut, Universität München
Version of record first published: 17 Oct 2011.

To cite this article: Erwin Knapek , Guy Lefranc , Wolfgang v. Gentzkow , Isolde Dietrich & Helmut Formanek (1983): Superconducting Lenses for Steric Structure Determination of Organic Material in the Electron Microscope, Molecular Crystals and Liquid Crystals, 96:1, 293-303

To link to this article: http://dx.doi.org/10.1080/00268948308074712

Mol. Cryst. Liq. Cryst., 1983, Vol. 96, pp. 293–303
0026-8941/83/9604–0293/$18.50/0

Printed in the United States of America

SUPERCONDUCTING LENSES FOR STERIC STRUCTURE DETERMINATION OF ORGANIC MATERIAL IN THE ELECTRON MICROSCOPE

ERWIN KNAPEK, GUY LEFRANC, WOLFGANG v. GENTZKOW, ISOLDE DIETRICH, HELMUT FORMANEK*
Zentrale Forschung und Entwicklung, Siemens AG, D-8000 München, Postfach 830 952
* Botanisches Institut, Universität München

Abstract The atomic structure of radiation sensitive organic material has been determined with a superconducting lens system for electron microscopes where the specimen is kept at a temperature of 4 K. Due to the high electromagnetic and mechanical stability of the instrument and due to the cryoprotection of organic specimens at low temperatures the "superconducting" electron microscope has been found to be very effective for this purpose.

INTRODUCTION

High resolution imaging in electron microscopy is a precondition for successful steric structure determination of organic material if X-ray methods are not applicable. In most cases, however, this imaging is prevented by the damage of the organic material due to the electron impact. The structure of unstained organic material is destroyed by an average dose of 100 e/nm^2 while 10^3 to 10^4 e/nm^2 are required for an electron micrograph with sufficient contrast. In most cases cooling of the specimen to 4K enhances the permissible dose by at least one order of magnitude. This low temperature is ensured by a superconducting lens system which, in addition, guarantees very high electrical and mechanical stability.

SUPERCONDUCTING LENS SYSTEM

Superconducting lens systems have been developed in our laboratory during the last decade. One of the systems has been installed in a test microscope with a 400 kV accelerator while another type (Fig. 1) can be attached to commercial microscopes with beam voltages up to 500 kV. The system consists of a cryostat with three concentrically arranged chambers for the cryogenic liquids e.g. nitrogen and helium. The inner helium chamber is only thermally connected with the intermediate helium dewar, and it contains the objective lens and at least one tightly connected intermediate lens. The objective lens is a superconducting shielding lens, i.e. unconventional material has been used for those parts of the lens which are producing the imaging field[2].

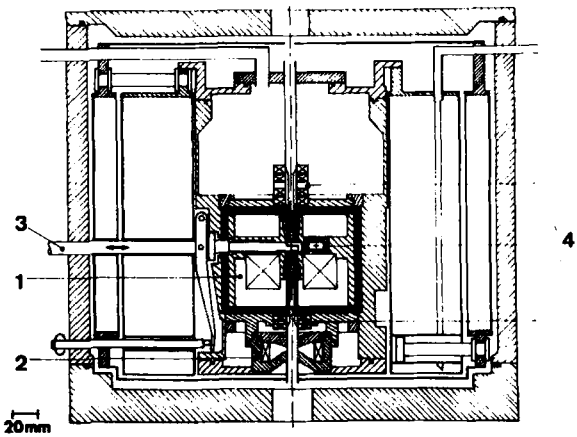

FIGURE 1 Superconducting lens system for a commercial microscope. 1 objective lens, 2 intermediate lens, 3 specimen holder, 4 stigmator and deflection coils.

A superconducting excitation coil wound with a NbTi multifilament wire is installed in a superconducting shielding

casing. The magnetic field on the optical axis is shaped by two superconducting shielding cylinders. The superconducting shielding material, composed of Nb-Sn-Cu sintermaterial with the effective superconducting phase Nb_3Sn screens the magnetic field so that only in the region of the lens gap the magnetic field can penetrate to the optical axis. Even electromagnetic stray fields outside the lens are totally screened off by the superconducting casing.

The intermediate lenses are iron circuit devices with superconducting excitation coils and all deflection and correction systems also consist of superconducting coils. The stigmator is installed in the lens gap and thus, a non rotational imaging field can be corrected directly. All lens coils and most of the correction coils can be operated in the persistent current mode such that disturbances and ripple of the current are eliminated. The current generator is switched off after the coil is excited to the desired value. The objective lens is equipped with a side entry specimen stage. After a coarse positioning of the specimen the holder is disconnected from the warmer parts of the cryostat. During the experiment the specimen can be shifted mechanically with a fine adjustment over lever arms with a reproducibility of about 50 nm. In general mechanical adjustments from outside are avoided as far as possible in order to minimize the heat-transfer into the lens system.

The lens gap in the system Fig. 1 is relatively large since the objective lens is operated with a high excitation. Some characteristic data from an electron microscope with a superconducting lens system are listed in table 1.

TABLE 1 Data for a superconducting two-lens system

Lens strength k^2 (second zone mode)	5
Focal length f	1.7 mm
Chromatic aberration constant	1.3 mm
Spherical aberration constant	1.2 mm
Basic astigmatism $\Delta f/f$	0.7 %
Gap	7.5 mm
Drift of specimen	0.03 nm/min
Positioning reproducibility of specimen	50 nm

CRYOPROTECTION AND SPECIMEN PREPARATION

Radiation damage, the most serious problem in high resolution electron microscopy of organic materials is caused by chemical bond breaking primarily due to the inelastic interaction of the electrons with the matter. Subsequent secondary effects are e.g. diffusion or migration of molecular fragments and evaporation of components with high vapor pressure so that after an irradiation with a high dose only a carbon skeleton is left. The goal was to discover if cryoprotection at 4 K permits high resolution imaging. This necessitates the determination of the dose which causes specimen destruction. For this the vanishing of electron diffraction patterns from crystalline material is mainly used. The diffraction patterns (Fig. 2) taken at 300 K and 4 K clearly demonstrate the existence of cryoprotection.

In order to obtain quantitative results, the dose D_e which causes a reduction of the intensity of the first order reflections by a factor 1/e is measured. Cryoprotection factors, i.e. values for D_e (300 K)/D_e (4 K) above 100 were published some time ago[1], but recently some of these values could not be reproduced. More thorough investigations were

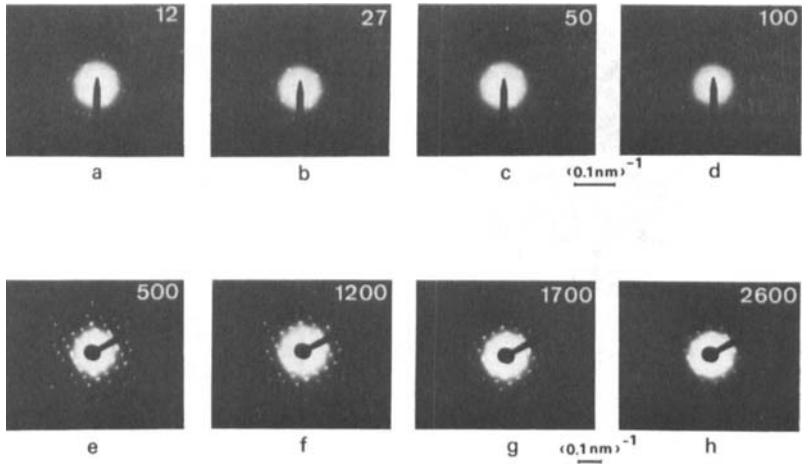

FIGURE 2 Electron diffraction patterns of phenylalanine. Decrease of the intensity of the reflections with increasing dose, a - d: 300 K, e - h: 4 K. The numbers give the accumulated dose in e/nm^2.

performed in order to find out the reasons for these discrepancies. The diffraction spots were spread on the photographic emulsion, so that errors in respect to densitometry were avoided. The studies confirmed that a reproducible specimen preparation method has not been found yet and that numerous changes in the object may happen during irradiation which prevent extraction of the D_e values from diffraction experiments. An example is demonstrated in Fig. 3 where the intensity of the reflections changes at random with increasing accumulated dose. We assume that tilting and bending of the specimen in the beam took place as sketched in Fig. 3. Such effects may easily occur if material with very low thermal and electrical conductivities at 4 K such as Formvar or collodium foils are used for support films. Even using carbon foils with considerable surface roughness which have

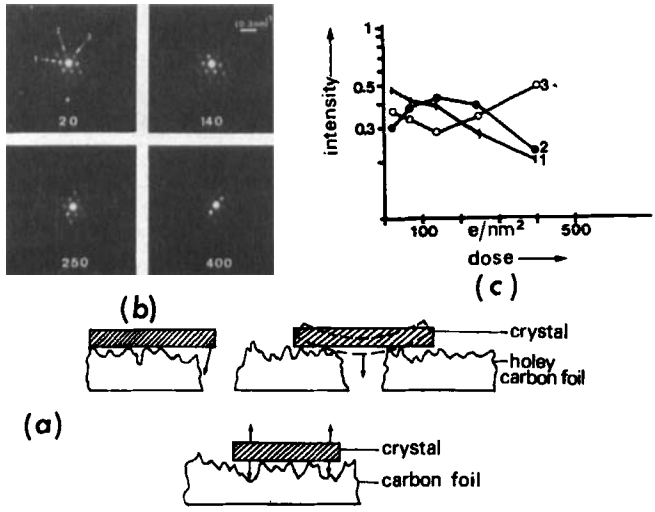

FIGURE 3 Changing of crystal position during irradiation demonstrated on l-valine (a) possibilities for tilting of the crystal, (b) electron diffraction patterns taken with increasing accumulated dose, (c) corresponding variation of intensity of the three marked reflections.

reasonable conductivity at 4 K, the contact resistance between carrier foil and crystal, which increases with the falling temperature, may be so much enhanced that heating and charging by the beam changes the specimen position. If the specimen is situated on a carbon foil near the copper bar of the carrier net, the thermal and electrical conduction is improved. The intensity of the first order reflections decays linearly with increasing accumulated dose in a semi-logarithmic plot as shown in Fig. 4. The D_e value is about an order of magnitude higher than at room temperature in this case. Until recently we obtained diffraction results given in Fig. 4 only by chance. Based on our experience we

can suggest the use of support films with not too low thermal and electrical conductivities or embedding the specimen in carbon foil (Fig. 5) or vitreous ice in order to improve the mechanical stability. A complete preparation method, however, for achieving reproducable results has not yet been worked out.

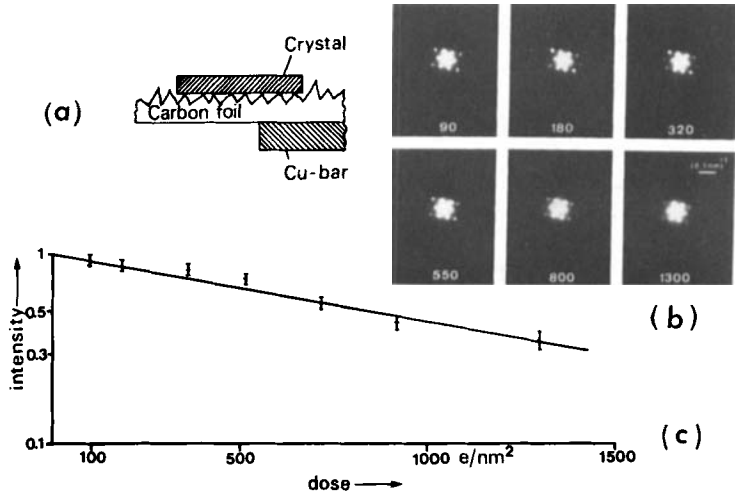

FIGURE 4 Fading of the intensity in the reflections caused only by radiation damage (a) position of l-valine crystal, (b) diffraction patterns taken with increasing dose and (c) densitometric evaluation

In spite of these difficulties we succeeded in taking direct high resolution images of radiation sensitive organic material (Table 2). In some cases the dose required for recognizing certain lattice fringes in the micrograph corresponded to the D_e value for the same periodicity in the diffraction patterns. The tolerable dose for direct imaging the most prominent lattice fringes of the embedded Cu-complex of BSH was even higher than the D_e value measured from electron diffraction patterns[3].

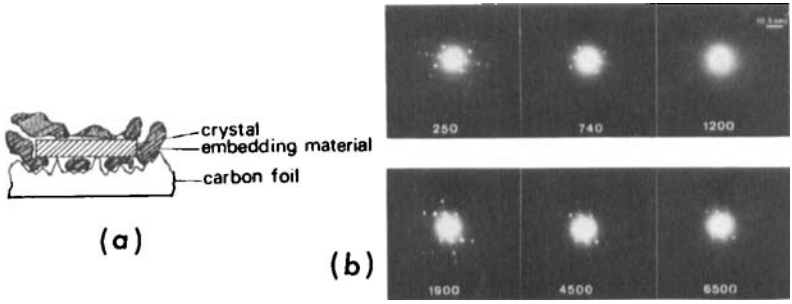

FIGURE 5 Influence of embedding on radiation damage of single crystals of calcium deoxicholate, (a) principle of embedding, (b) electron diffraction patterns, above: without embedding and below: with embedding.

TABLE 2 Direct images obtained with superconducting lenses

Material	Support film	Dose for imaging e/nm^2	Dose rate $e/nm^2 . s$	Resolved distance nm	Specimen prepared by
Hexaphenylene mercury	aluminum oxide			0.36	H. Formanek
Murein	graphite oxide	3.10^5	300	0.45,0.22	H. Formanek
Catalase	carbon	1000	15	1.2	W. Chiu
$(Cu_2BSH)_n$	carbon	3.10^4	100	1.1,0.9	H. Formanek
Cellulose	carbon	1000	80	0.54	H. Chanzy
Paraffin	carbon	3000	100	0.41,0.37	D. Dorset
Coronene	carbon	9500		0.7	J.R. Fryer
Purple membrane	carbon	2000	20	0.7	D. Studer
Crotoxin	carbon	1200	15	0.4	W. Chiu

STERIC STRUCTURE DETERMINATION OF THE COPPER COMPLEX OF BSH

BSH (N,N'-bissalicyloylhydrazine) is known as one of the best copper deactivators which prevents the accelerated thermooxidative aging of polyolefin insulation material

by copper catalysis[4]. Before we started our experiments it was only known that the deactivation of the copper ions is caused by formation of a completely inactive complex. Preliminary experiments have indicated that the complex is nearly amorphous. By addition of ammonia, however, crystals with linear dimensions of a few micrometers[5] could be obtained which were too small for performing a complete structure analysis by X-ray methods.

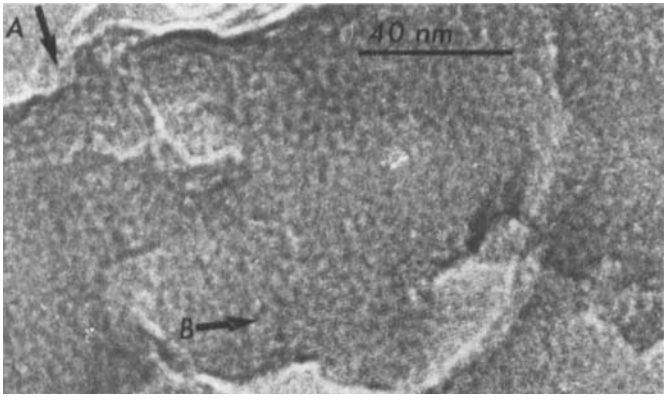

FIGURE 6 Direct image of $(Cu_2BSH)_n$. A:0.9 nm, B:1.1 nm

Conventional electron microscopy could not be applied since the crystals turned out to be very beam sensitive. We only succeeded in taking electron diffraction patterns, where the first and second order deflections were visible, which vanished at a dose of 500 e/nm^2. Diffraction experiments were performed in our "superconducting" microscope, where the specimen temperature is 4 K. High order reflections could be detected even if the accumulated dose was increased above 10^4 e/nm^2. In addition high resolution images could be taken with doses of 3.10^4 e/nm^2, where 0.9 and 1.1 nm lattice

fringes could be clearly recognized (Fig. 6)[5]. These periodicities can be correlated to the most intensive reflections of the diffraction patterns. With the help of such patterns under different Bragg-conditions and the electron micrographs a model of the complex could be constructed. Under the assumption of a planar structure of BSH a limited range of mutual orientations of these molecules crosslinked with one Cu-atom could be estimated. With regard to the allowed orientations, three dimensional packing models have been constructed and their Fourier transforms were iteratively fit to the electron diffraction patterns (Fig. 7a and b). These procedures resulted in the model Fig. 8.

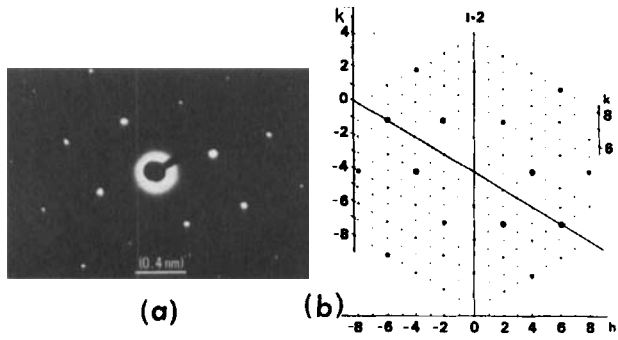

FIGURE 7 (a) Diffraction pattern of $(Cu_2BSH)_n$ and (b) corresponding Fourier transform of the model.

CONCLUSION

The example of the steric structure determination has shown that electron microscopy at 4 K will probably become one of the most powerful methods for this purpose on organic material. A superconducting lens system guarantees an object temperature of 4 K necessary for cryoprotection and in addition a very high electromagnetic and mechanical stability, and high resolution. Some problems in connection with specimen

preparation for 4 K electron microscopy have to be solved in the future in order to make the use of the microscopes more effective.

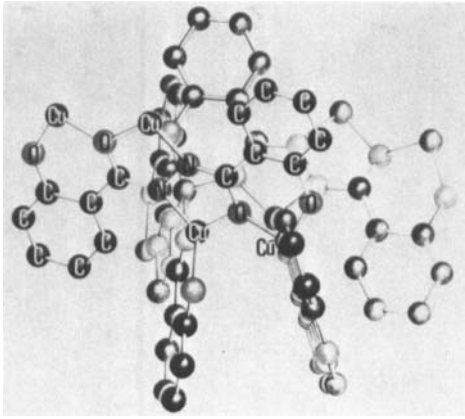

FIGURE 8 Model of $(Cu_2BSH)_n$

REFERENCES

1. J. Dubochet and E. Knapek, Chemica Scripta, 14, 267 (1978/79).
2. G. Lefranc and K. Nachtrieb, in Inst. Phys. Conf. Ser. Nr. 52, edited by T. Mulvey (The Inst. of Phys. London, 1982), p. 31-34
3. E. Knapek, H. Formanek, G. Lefranc and I. Dietrich, in 39th Ann. Proc. Electron Microscopy Soc. Amer., edited by G. W. Bailey (Claitor's Publ. Div. Baton Rouge, 1981), p. 22-23.
4. W. v. Gentzkow and D. Pieper, Siemens Forsch. Entwickl. Ber., 8, 309 (1979).
5. I. Dietrich, H. Formanek, W. v. Gentzkow and E. Knapek, Ultramicroscopy, 9, 75 (1982).